1973ApJ...183..441H

THE ASTROPHYSICAL JOURNAL, **183**:441–448, 1973 July 15
© 1973. The American Astronomical Society. All rights reserved. Printed in U.S.A.

MEASUREMENTS OF THE H_2CO 6-CENTIMETER EXCITATION TEMPERATURE. I. DARK DUST CLOUDS

CARL HEILES
Department of Astronomy, University of California, Berkeley
Received 1972 December 18

ABSTRACT

Highly accurate H_2CO 6-cm line profiles were observed in 14 positions located in dark dust clouds. Analyses of the relative strengths of the hyperfine components showed no anomalies. Therefore, excitation temperatures were derived for 10 positions which exhibited measurable saturation due to optical-depth effects. Nine of these positions have nearly the same excitation temperature, about 1.6° K. The other position definitely has a higher excitation temperature, about 2.2° K; this position is located in a cloud whose kinetic temperature is 18° K, substantially hotter and also probably denser than the "usual" dark dust cloud.
Subject headings: molecules, interstellar — nebulae — radio lines

I. INTRODUCTION

The 6-cm H_2CO line nearly always appears in absorption, even in the absence of a background radio source. In such cases, absorption occurs against the isotropic microwave background. This phenomenon can occur only if the excitation temperature of the 6-cm line is less than the brightness temperature of the microwave background itself, taken here as 2.8° K. In dark dust clouds (Palmer *et al.* 1969) the line has never been seen in emission.

This paper presents measurements of the excitation temperature in a number of dust clouds; preliminary results were given earlier by Heiles (1971). The method used is the same used previously for OH by Heiles (1969) and Turner and Heiles (1971). It involves comparing the observed intensities of hyperfine lines having the same excitation temperature and a known ratio of optical depth. In the case of OH these are two components of the 18-cm Λ doublet. The same method can, in principle, be used for the 6-cm line of H_2CO which consists of six hyperfine components, rather closely spaced in frequency. In practice the method is suitable only for cases in which the Doppler line width is small enough so that the hyperfine structure is not excessively smeared.

II. SELECTION OF POSITIONS

The Hat Creek 85-foot (26-m) telescope was equipped with a two-stage cooled parameter amplifier with system temperature about 55° K, and the 100-channel filter bank with channels of width and spacing 2 kHz. In the spring of 1971 a survey of 44 positions in eight dust clouds was performed in an attempt to map their kinematical structure, spending about 2 hours on each position. From this preliminary survey 14 positions showing the strongest lines were selected, with due regard for sampling different clouds. These positions were then observed intensively for 20 to 60 hours apiece.

Such long integrations are necessary to achieve a suitably high signal-to-noise ratio for a reliable determination of the excitation temperature T_x (see § III). For this reason the selection of positions is strongly biased toward those with the most intense lines. Because they do not compose a random sample, it is possible that the derived

© American Astronomical Society • Provided by the NASA Astrophysics Data System

1973ApJ...183..441H

excitation temperatures are not generally representative. For this sample there was no evidence for anomalous hyperfine intensities, as reported for one dust cloud by Dieter (1972); however, see Heiles and Turner (1973).

III. LEAST-SQUARES ANALYSIS AND RESULTS

a) *Theory*

The equation of transfer, which provides the emergent brightness temperature $T_{B(f)}$ (a function of frequency f) from a cloud having excitation temperature T_x and optical depth $\tau_{(f)}$ in some microwave line, is

$$T_{B(f)} - T_c = (T_x - T_c)[1 - \exp(-\tau_{(f)})], \tag{1}$$

where T_c is the continuum brightness temperature behind the cloud. For a frequency-switched system the observed quantity is the antenna temperature, equal to the left-hand side of this equation multiplied by F/η_b. The quantity η_b is the beam efficiency; F is a factor near unity, equal to the appropriately weighted fractional area of the telescope beam occupied by the cloud.

In the case of H_2CO, five of the six hyperfine components have very nearly the same frequency. The sixth (the $1 \rightarrow 0$ component) is displaced by about 18 kHz (equivalent to 1.1 km s^{-1}). Each of these components produces its own Doppler-broadened line profile. Astronomical velocities in dust clouds are large enough to blend the five neighboring components into one line, but usually small enough to keep the sixth distinct.

We assume in this paper that the velocity profile is Maxwellian. In this case the optical depth as a function of frequency is given by

$$\tau_{(f)} = A \times \sum_{i=1}^{6} \alpha_i \exp[-(f - f_i - F)^2/\Delta^2], \tag{2}$$

where A is the central optical depth of the $2 \rightarrow 2$ component, F the central frequency of the $2 \rightarrow 2$ component, the α_i are the relative optical depths, and the f_i are the relative frequencies of the six hyperfine components (Tucker *et al.* 1971). The $2 \rightarrow 2$ component is used as the standard because it is the most intense.

It is then appropriate to obtain the excitation temperature T_x and optical depth A by a least-squares fit of equations (1) and (2) to the observed profile. In some cases two velocity components were required to represent the observed profiles; therefore, in general, the observed profiles were fit with a function of the form

$$T_{A(f)} = K + \sum_{j=1}^{N} (T_{x_j} - T_c)[1 - \exp(-\tau_{(f)})] \tag{3}$$

using the least-squares technique (Chauvenet 1874), where T_A is the antenna temperature and N is the number of velocity components, equal to 1 or 2 in the present paper. The constant term K is included to account for small zero-level errors. The quantity T_c was always taken as 2.8° K, assuming negligible galactic continuum radiation. This should be generally valid because the observed positions are all well away from the galactic plane (see Heiles 1969); however, a small continuum excess cannot be ruled out for every position since no continuum measurements were performed.

b) *Practice*

The values of the derived parameters, and other essential data, are given in table 1.

We illustrate the observed line shapes, residuals, and difficulties involved in the figures. Figure 1 shows the narrowest line observed; the hyperfine structure is clearly

© American Astronomical Society • Provided by the NASA Astrophysics Data System

1973ApJ...183..441H

TABLE 1

POSITIONS AND DERIVED QUANTITIES

Position	R.A.$_{1950}$	Decl.$_{1950}$	l^{II}	b^{II}	F (see eq. [1])	T_x (° K)	A	V (km s^{-1})	ΔV (km s^{-1})	Kinetic Temperature (° K)†
1..........	04^{h}20^{m}35^s	24°58′	172°09	−16°94	0.58	1.19 ± 0.21	0.68 ± 0.15	7.050 ± 0.007	0.305 ± 0.014	...
						...	...	5.0[a]	0.5[a]	...
2[b].........	04 26 09	24 32	173.31	−16.28	0.76	...	...	6.40 ± 0.007	0.417 ± 0.009	...
						...	...	4.23 ± 0.063	0.340 ± 0.087	...
3[c]..........	04 29 00	24 23	173.87	−15.89	0.85	...	...	6.587 ± 0.050	0.540 ± 0.047	...
						...	...	5.683 ± 0.016	0.370 ± 0.016	...
4..........	04 30 14	26 12	172.64	−14.49	1.00*	2.11 ± 0.16	0.58 ± 0.21	6.159 ± 0.014	0.394 ± 0.025	...
5[d].........	04 34 46	26 09	173.36	−13.75	0.85	≤1.60	≤0.3	6.470 ± 0.012	0.400 ± 0.019	6
						...	...	5.281 ± 0.122	0.598 ± 0.193	...
6..........	04 36 46	25 41	174.03	−13.71	0.76	1.63[e] ± 0.10	0.67 ± 0.11	6.239 ± 0.007	0.518 ± 0.019	6
						...	...	5.0[f] ± 0.1	0.5 ± 0.1	...
7[g].........	04 38 07	25 24	174.45	−13.66	0.83	...	...	5.966 ± 0.041	0.718 ± 0.101	6
						1.96 ± 0.17	0.73 ± 0.22	5.363 ± 0.006	0.209 ± 0.014	...
8[h].........	15 50 54	−04 31	4.145	35.759	0.91	1.69 ± 0.14	0.55 ± 0.10	2.795 ± 0.006	0.352 ± 0.011	6
9[i]..........	15 51 28	−02 46	5.967	36.736	0.63	1.64 ± 0.09	0.81 ± 0.13	2.536 ± 0.009	0.421 ± 0.015	...
10[j]..........	16 24 09	−24 28	353.05	16.67	1.00	2.22 ± 0.02	1.25 ± 0.13	3.788 ± 0.009	0.660 ± 0.022	18
11[k].........	16 29 35	−24 24	353.949	15.780	0.86	1.39 ± 0.41	0.34 ± 0.15	4.030 ± 0.010	0.518 ± 0.026	...
12[l]..........	16 45 00	−11 55	6.66	20.63	0.79	1.72 ± 0.20	0.43 ± 0.12	3.897 ± 0.007	0.607 ± 0.025	...
13[m].........	22 27 47	74 58	114.08	14.87	1.11	2.39 ± 0.25	0.32 ± 0.28	−4.036 ± 0.017	0.610 ± 0.060	5
14[n].........	22 35 47	74 58	114.54	14.60	1.30	≤2.45	≤0.8	−4.303 ± 0.015	0.763 ± 0.015	6

* Assumed, not measured. † From Heiles (1969), and/or Penzias *et al.* (1972).

[a] Eye estimated. Intensity ~10 percent of the other components.

[b] $(T_x - 2.8)A = -0.79 \pm 0.01$; $(T_x - 2.8)A = -0.08 \pm 0.02$.

[c] $(T_x - 2.8)A = -0.41 \pm 0.02$; $(T_x - 2.8)A = -1.05 \pm 0.05$.

[d] $(T_x - 2.8)A = -0.46 \pm 0.01$; $(T - 2.8)A = -0.05$; in cloud 2 of Heiles (1968).

[e] In cloud 2. Trustworthy despite two velocity components.

[f] Eye estimated. Intensity ~5 percent of the other components.

[g] $(T_x - 2.8)A = -0.29$; in cloud 2. Untrustworthy because of two velocity components.

[h] In cloud L134 of Heiles (1968). [i] In a dark cloud located near cloud L134.

[j] In cloud 4 of Heiles (1968). [k] In a dark cloud located near cloud 4.

[l] In cloud 5 of Heiles (1968).

[m] In cloud 1 of Heiles (1968); error is too big for a good estimate of T_{ex}.

[n] In cloud 1.

© American Astronomical Society • Provided by the NASA Astrophysics Data System

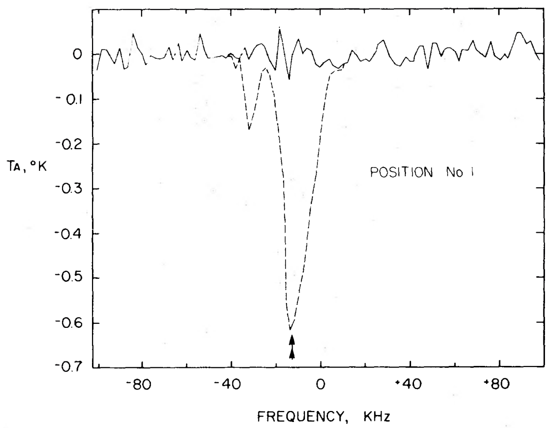

FIG. 1

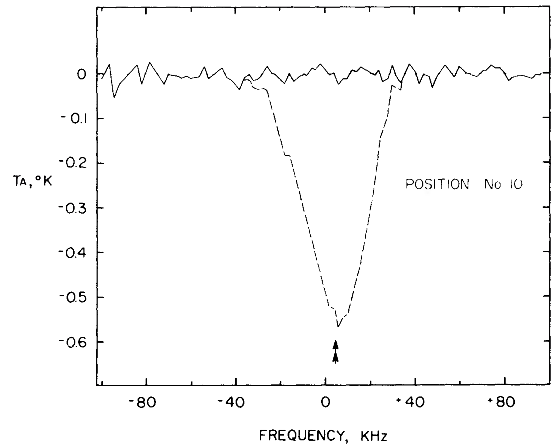

FIG. 2

FIG. 1.—Results for position 1 (table 1). *Dashed line*, the observed spectrum; *solid line*, residuals from best fit. This profile is the narrowest observed, and the $1 \rightarrow 0$ hyperfine component is clearly apparent at about -30 kHz. The arrow indicates the central frequency of the $2 \rightarrow 2$ component.

FIG. 2.—Results for position 10 (table 1). *Dashed line*, the observed spectrum; *solid line*, residuals from best fit. This profile is the widest observed for which a good least-squares fit was made. Although the $1 \rightarrow 0$ hyperfine component is not clearly distinct, its effects are evident in the asymmetry of the line. The arrow indicates the central frequency of the $2 \rightarrow 2$ component.

apparent. Figure 2 shows the widest line for which accurate results could be obtained. While the $1 \rightarrow 0$ hyperfine component is not clearly distinct, its effects are obvious in the asymmetry of the line, and equation (3) is fitted to the data without difficulty (due partly to an unusually large optical depth at this position). Wider velocity dispersions lead to unacceptably large errors in the derived quantities; a case in point is position number 14 (see table 1).

In practice, the method works by comparing the intensity of the one "line" consisting of the blend of the closely spaced five hyperfine components with the intensity of the $1 \rightarrow 0$ hyperfine component. Thus the noise must be small compared to the intensity of the $1 \rightarrow 0$ component. This is a rather severe requirement.

Figure 3 shows a line which is composed of two velocity components. It so happens that the separation of these components is 0.9 km s^{-1}, nearly equal to the 1.1 km s^{-1} separation of the $1 \rightarrow 0$ component from the blended line of the other five hyperfine components. It is therefore tempting to interpret this profile as a single velocity component with a very large optical depth A. However, an attempt to fit this profile with a single velocity component leads to the residuals shown in figure 3, which systematically depart from zero in the vicinity of the line and are obviously unacceptable. These residuals occur because the line is really composed of two velocity components which differ by 50 percent in their widths (see table 1). Moreover, examination of the profile with an optimistic eye shows the presence of the $1 \rightarrow 0$ hyperfine component associated with the second velocity component, appearing near a frequency of -28 kHz.

Although cases with $N = 2$ such as this can be fitted with equation (3), and values derived for T_x and A for each velocity component, the derived values are obviously untrustworthy. In the presence of noise on the profile, it is impossible for the mathematical procedure to reliably distinguish an optical-depth effect from the intensity of the second velocity component when the separation is of the order of 18 kHz. For this reason some of the results for positions having two velocity components should be accepted with circumspection; these are so indicated.

© American Astronomical Society • Provided by the NASA Astrophysics Data System

1973ApJ...183..441H

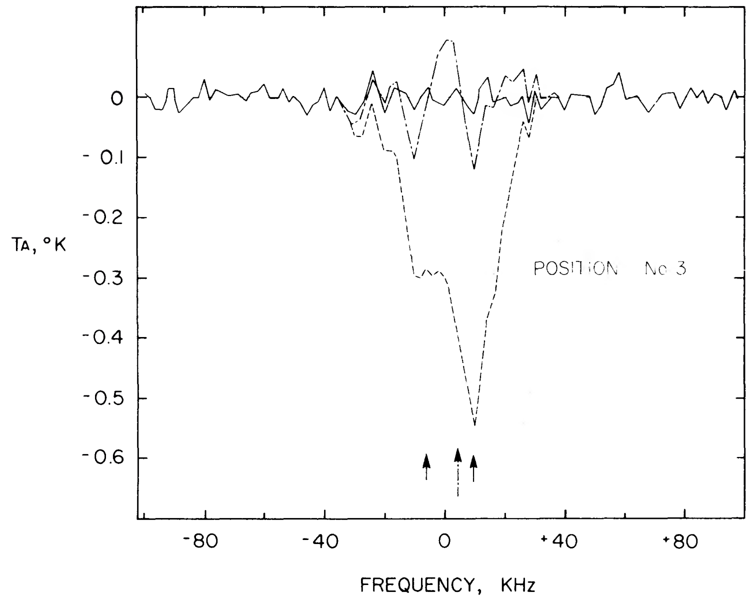

FIG. 3.—Results for position 3 (table 1). *Dashed line*, the observed spectrum; *dash-dot line*, residuals from a best fit with one velocity component; *solid line*, residuals from best fit with two velocity components. The dash-dot arrow indicates the central frequency of the $2 \rightarrow 2$ component for the unacceptable single velocity component; the solid arrows indicate the central frequencies of the $2 \rightarrow 2$ components for the double velocity component fit. The $1 \rightarrow 0$ component of the lower-frequency velocity component is visible near -30 kHz.

c) The Quoted Errors

The errors quoted are the mean errors as defined by Chauvenet (1874): if a large number of measurements equivalent to the one already existing at each position were taken, the true errors δ of the derived values would be distributed as $\exp(-\delta^2/2\sigma^2)$, where σ is the mean error. Therefore, the quoted errors are not strict bounds on the derived quantities. However, if the errors are multiplied by a suitable factor, say 3, they do then represent strict bounds for all practical purposes. This statement was confirmed experimentally for the optical depth by modifying the fitting program to solve for T_x, F, and Δ with A specified and held fixed. The residuals were plotted for several values of A surrounding the value quoted in table 1, and when the specified value of A differed by a factor of 3 times the error quoted in table 1 the residuals were quite unacceptable to visual inspection. Also evident, as expected, was the fact that an attempt to define strict bounds must account for the nonlinearity in equation (3) by assigning errors which differ for + and − deviations from the derived quantities quoted in table 1. We regard the application of a factor of 3 to yield approximate estimates of maximum errors in all quantities.

Connoisseurs of least-squares fitting will recognize that the traditional (Chauvenet 1874) methods involving linearized Taylor expansions about an assumed solution of equation (3) will be unsuccessful for small τ (or, equivalently, A; see eq. [2]). This results from the fact that $e^{-\tau} \rightarrow 1 - \tau$ as $\tau \rightarrow 0$, and the equation becomes degenerate with respect to $(T_x - 2.8)$ and τ. The product of $(T_x - 2.8)$ and A is then indicative of the line intensity and is therefore a quite well-defined negative number; however, the derived values of either of the two quantities may be negative and their derived errors far too large for consistency with linearized expansions. Their derived values are then completely meaningless. For example, one solution for position 14 yielded $(T_x - 2.8) = 1.3 \pm 2.4$ and $A = -0.15 \pm 0.25$. In such cases only upper limits on

© American Astronomical Society • Provided by the NASA Astrophysics Data System

1973ApJ...183..441H

T_x and A can be derived, but not in the usual manner. Instead, we used the modified version of the program discussed in the above paragraph and solved for T_x with a number of specified values of A, plotting the 100 residuals in the spectrum in each case. We picked the upper limit for A as that value which produced residuals which appeared visually unacceptable; the upper limit for T_x is the associated value derived for T_x. These upper limits, then, represent strict bounds—or very nearly so. (However, the errors quoted for the velocity and velocity width for these cases are defined in the usual way.)

Apart from errors derived from the residuals of the least-squares fit, which are random in character and average to zero with a large number of observations, systematic errors exist. There are three obvious sources of systematic error. The first results from the fact that the 100 filters in the receiver all have slightly different shapes; furthermore, they do not sample an infinitesimally narrow bandwidth, as assumed by the least-squares fitting program used for this paper. This results in residuals which do not decrease with integration time, and which are most deleterious for narrow lines; they are noticeable in figure 1. These will cause slight errors in the derived quantities, particularly the velocity and velocity width. However, the errors should be less than a few percent in width and a few hundredths of a km s^{-1} in velocity.

The second concerns only the derived excitation temperatures; it is the uncertainty in the ratio F/η_B (see discussion following eq. [1]). The beam efficiency was determined using the value of the noise-calibration tube measured in the laboratory (38° K), deriving the aperture efficiency (63 percent) and half-power beamwidth (11.1′) on Cas A (assumed 843 f.u. in the spring of 1972, see Scheuer and Williams 1968), and using the standard relations (Mezger and Henderson 1967) to obtain beam efficiency (100 percent). Although the derived beam efficiency is extraordinarily high, its value is directly proportional to the value of the noise tube used in the calculation. This value could easily be in error by 10 percent. Nevertheless, because the antenna-temperature scale is also proportional to the value of the noise tube, the final brightness-temperature scale is independent of the assumed value of the noise tube. It can be in error only by an error in the assumed flux of Cas A, or if the ratio of Cas A to noise tube, or the half-power beamwidth, were measured incorrectly. We estimate these sources of error to contribute less than 7 percent error to the final scale of brightness temperature. An additional uncertainty of 5 percent exists because the system-gain calibration was not performed continuously during observations. Hence, the total error in intensity scale is less than 12 percent; this directly affects the brightness-temperature scale which is proportional to $T_x - 2.8$.

However, the factor F which represents the fractional area of the beam filled by the cloud is rather poorly known. For each position it was determined by observing four positions surrounding the central one, displaced by 0°1. The intensities of the four surrounding positions were averaged, and F taken equal to the ratio of the intensity of the average of the four positions divided by that of the central position. This procedure is not particularly satisfactory unless the derived value of F is close to unity, as it is for most of the positions. However, for position 1 in table 1, F was found to be 0.58, too small for this procedure to yield acceptable results. Examination of this cloud on the Palomar prints would suggest a value of F closer to 0.75 if H_2CO is well correlated with optical extinction. The derived values of T_x are not simply proportional to the value of F, because the value of F affects the brightness-temperature scale which is proportional to $T_x - 2.8$. Therefore, if F were really 0.75 for position 1, the derived value of T_x would rise to 1.45° ± 0.17° K. Position 9 might also be affected in this way.

A third type of error is unrelated to observing procedure or equipment but instead results from the inadequacy of equations (2) and (3) to accurately describe the true physical situation. Two of the more obvious such discrepancies are the possible non-Maxwellian line shape and the variation of T_x along the line of sight. We believe the

© American Astronomical Society • Provided by the NASA Astrophysics Data System

1973ApJ...183..441H

first to be of little importance, because in no case have the residuals of the least-squares fit been found to indicate that a Maxwellian line shape is anything but perfectly satisfactory. The second may possibly be important and would result in our deriving a weighted average for T_x along the line of sight. Some numerical examples are given by Dieter (1973). Hence, values of T_x quoted in table 1 may be higher than the lowest values attained along the line of sight.

IV. CLOUD 4, THE RARA AVIS

Examination of the results in table 1 reveals that with due consideration of the magnitude and meaning of the quoted errors (§ III), all positions but number 10 may have the same value of T_x. The average for the seven reliable determinations not including position 10 is 1.62° K. Positions 1 and 4 depart from this average by enough to be possibly significant, but not necessarily so.

Position 10, located in cloud 4 of Heiles (1968), is a definite exception, with $T_x = 2.22° \pm 0.02°$ K. The distinctly different result for T_x in cloud 4 requires a detailed discussion of its validity with regard to extraneous effects. As discussed in § III, the existence of additional velocity components can produce incorrect values for the derived value of T_x. However, in the central parts of cloud 4 there is no known evidence for more than one velocity component. Although the velocity dispersion is larger than for the typical cloud examined in this paper, it is not so large as to obscure the asymmetry arising from the $1 \rightarrow 0$ hyperfine component. The derived value of T_x has an extraordinarily small error. This results from the nonlinear coupling in equation (3) of T_x to the optical depth A. When A is large, as it is for this position, T_x becomes extremely well determined. Finally, $F = 1$ for this position. We can find no reason to distrust this result, nor its associated error. Since the validity of the result for cloud 4 seems unassailable, we conclude that T_x is not always the same in dust clouds.

Cloud 4 is thought to be different in that its kinetic temperature is about 18° K rather than the 5°–6° K which, on the basis of an admittedly quite limited sample, seems more typical for dust clouds according to the results of Heiles (1969) and Penzias *et al.* (1972), which are summarized in table 1. The constancies of T_x and kinetic temperature apart from cloud 4 are quite remarkable. It is tempting to conclude, therefore, that the higher T_x measured for cloud 4 is a direct result of the higher kinetic temperature which is known to exist in this cloud, rather than other causes such as a difference in H_2 density. This conclusion is hardly definitive, however, because gas densities in dust clouds are difficult to measure. Turner (1972) feels that the gas density in cloud 4 may be somewhat larger than in other dust clouds on the basis of enhanced abundances of complex molecules.

Townes and Cheung (1969) proposed collisional refrigeration of the H_2CO 6-cm lines, obtaining numerical estimates of its effectiveness by use of a hard-sphere classical model. They find that refrigeration occurs quite generally. However, their equation (6) predicts only a small change in T_x as the kinetic temperature changes from 6° to 18° K. On the other hand, Thaddeus (1972*a*) treated collisional refrigeration quantum-mechanically by use of the sudden approximation and found refrigeration cannot occur for kinetic temperatures lower than 35° K. There is some question, however, whether this approximation is adequate. Thaddeus and Solomon alternatively propose that refrigeration occurs from deviations of the isotropic microwave background from a thermal spectrum near $\lambda = 2$ mm (see Thaddeus 1972*b*, for a brief description). If this is correct, dependence of T_x on kinetic temperature could occur only if the collisional-excitation rates were not completely negligible with respect to radiative-refrigeration rates. However, radiative refrigeration appears difficult to accept in view of the recent detection of the 2-cm line ($J = 2$ state) in absorption, which can be understood only if the microwave background has quite substantial

© American Astronomical Society • Provided by the NASA Astrophysics Data System

1973ApJ...183..441H

deviations from a thermal spectrum near $\lambda = 1$ mm (Evans 1972). Finally, Litvak (1970) has proposed refrigeration by infrared-emission lines generated in shock-heated layers of a gravitationally collapsing cloud. This mechanism predicts a higher T_x for higher kinetic temperature, in accord with the present observational results. However, it also predicts dependence of T_x on the collapse velocity and the solid angle of the shock-heated layer as seen by the molecule; this would seem to be in contradiction to the near constancy of T_x for the remaining positions of table 1. Evidently, the theoretical situation is unsatisfactory; and from the observational side, accurate estimates of gas density are required.

This work was supported by the National Science Foundation.

REFERENCES

Chauvenet, W. 1874, *A Manual of Spherical and Practical Astronomy* (Philadelphia: Lippincott), p. 469.
Dieter, N. H. 1972, *Ap. J.* (*Letters*), **178**, L133.
———. 1973, *Ap. J.*, **183**, in press.
Evans, N. 1972, personal communication.
Heiles, C. 1968, *Ap. J.*, **151**, 919.
———. 1969, *ibid.*, **157**, 123.
———. 1971, NRAO Molecular Symposium, Charlottesville, Va.
Heiles, C., and Turner, B. E. 1973, *Ap. J.* (*Letters*), submitted.
Litvak, M. M. 1970, *Ap. J.* (*Letters*), **160**, L133.
Mezger, P., and Henderson, A. P. 1967, *Ap. J.*, **147**, 471.
Palmer, P., Zuckerman, B., Buhl, D., and Snyder, L. E. 1969, *Ap. J.* (*Letters*), **156**, L147.
Penzias, A. A., Solomon, P. M., Jefferts, K. B., and Wilson, R. W. 1972, *Ap. J.* (*Letters*), **174**, L43.
Scheuer, P. A. G., and Williams, P. J. S. 1968, *Ann. Rev. Astr. and Ap.*, **6** 321.
Thaddeus, P. 1972*a*, *Ap. J.*, **173**, 317.
———. 1972*b*, *Ann. Rev. Astr. and Ap.*, **10**, 305.
Townes, C. H., and Cheung, A. C. 1969, *Ap. J.* (*Letters*), **157**, L103.
Tucker, K. D., Tomasevich, B. R., and Thaddeus, P. 1971, *Ap. J.*, **169**, 429.
Turner, B. T. 1972, private communication.
Turner, B. T., and Heiles, C. 1971, *Ap. J.*, **170**, 453.

© American Astronomical Society • Provided by the NASA Astrophysics Data System